

**Dhirendra K. Simanshu and
 M. R. N. Murthy***

Molecular Biophysics Unit, Indian Institute of
 Science, Bangalore, India

Correspondence e-mail: mrn@mbu.iisc.ernet.in

Received 16 September 2004

Accepted 18 October 2004

Online 23 October 2004

Cloning, expression, purification, crystallization and preliminary X-ray diffraction analysis of propionate kinase (TdcD) from *Salmonella typhimurium*

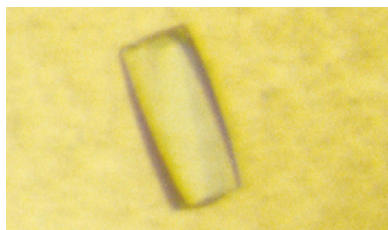
In the cell, propionate is mainly formed during β -oxidation of odd-numbered carbon-chain fatty acids, fermentation of carbohydrates and degradation of the amino acids threonine, valine, isoleucine and methionine. Recently, it has been shown that L-threonine is non-oxidatively cleaved to propionate *via* 2-ketobutyrate. The last step in this process, conversion of propionyl phosphate and ADP to propionate and ATP, is catalysed by propionate kinase (EC 2.7.1.-). Here, the cloning of propionate kinase (molecular weight 44 kDa) from *Salmonella typhimurium* with an N-terminal hexahistidine affinity tag and its overexpression in *Escherichia coli* are reported. Purified propionate kinase was found to cocrystallize with ADP in the hanging-drop vapour-diffusion and microbatch methods. Crystals belong to space group $P3_121$ or $P3_221$, with unit-cell parameters $a = b = 111.47$, $c = 66.52$ Å. A complete data set to 2.2 Å resolution has been collected using an image-plate detector system mounted on a rotating-anode X-ray generator.

1. Introduction

After acetate, propionate is the second most abundant low-molecular-weight carbon compound found in soil. Many aerobic microorganisms as well as some anaerobes are able to utilize propionate as a sole carbon and energy source. Propionate is mainly formed during the β -oxidation of odd-numbered carbon-chain fatty acids, the fermentation of carbohydrates, the oxidative degradation of the branched-chain amino acids valine and isoleucine and from the carbon skeletons of threonine, methionine, thymine and cholesterol. Studies of the degradation of these amino acids in *Escherichia coli* have revealed that several enzymes that utilize diverse catalytic mechanisms are involved in these pathways. Recently, the anaerobically regulated *tdc* operon has been shown to encode a metabolic pathway for the degradation of serine and threonine (Sawers, 1998).

In *E. coli*, the anaerobically regulated *tdcABCDEFGG* operon encodes proteins involved in the transport and fermentation of L-serine and L-threonine (Hesslinger *et al.*, 1998). Induction of the *tdc* operon occurs under anaerobic conditions in the presence of the amino acids serine, threonine, valine or isoleucine as well as fumarate and cyclic AMP (Schweizer & Datta, 1988). Enzymes encoded by the *tdc* operon lead to the production of energy-rich keto acids that are subsequently catabolized to produce ATP *via* substrate-level phosphorylation (Hesslinger *et al.*, 1998; Sawers, 1998). Tentative functional roles have been assigned to six of the seven gene products of the *tdc* operon. TdcA is a *trans*-acting positive regulator (Ganduri *et al.*, 1993; Sawers, 2001), TdcB is a threonine dehydratase (Datta *et al.*, 1987), TdcC is an integral membrane protein associated with the transport of serine and threonine (Sumantran *et al.*, 1990), TdcD is a propionate kinase (Hesslinger *et al.*, 1998), TdcE is a keto formate lyase (Hesslinger *et al.*, 1998) and TdcG is a serine dehydratase (Hesslinger *et al.*, 1998), while the function of the protein encoded by TdcF is unknown (Hesslinger *et al.*, 1998).

In *E. coli*, L-threonine is catabolized *via* 2-ketobutyrate. Although the enzymatic conversion of threonine to propionate had been demonstrated as early as 1963 in cell-free extracts of *Clostridium tetanomorphum* (Tokushige *et al.*, 1963), the metabolic fate of 2-ketobutyrate remained enigmatic for a long time. Van Dyk & LaRossa (1987) proposed that in *Salmonella typhimurium* 2-keto-



butyrate was oxidatively decarboxylated to propionyl-CoA by a thiamine-dependent enzyme. Recently, it has been shown in *E. coli* that 2-ketobutyrate can also be non-oxidatively cleaved to propionate (Fig. 1) by pyruvate formate lyase or by keto-acid formate lyase, phosphotransacetylase and propionate kinase (Hesslinger *et al.*, 1998). The final reaction in this process, the conversion of propionyl phosphate and ADP to propionate and ATP, is catalyzed by propionate kinase (TdcD). Propionate kinase exhibits an amino-acid

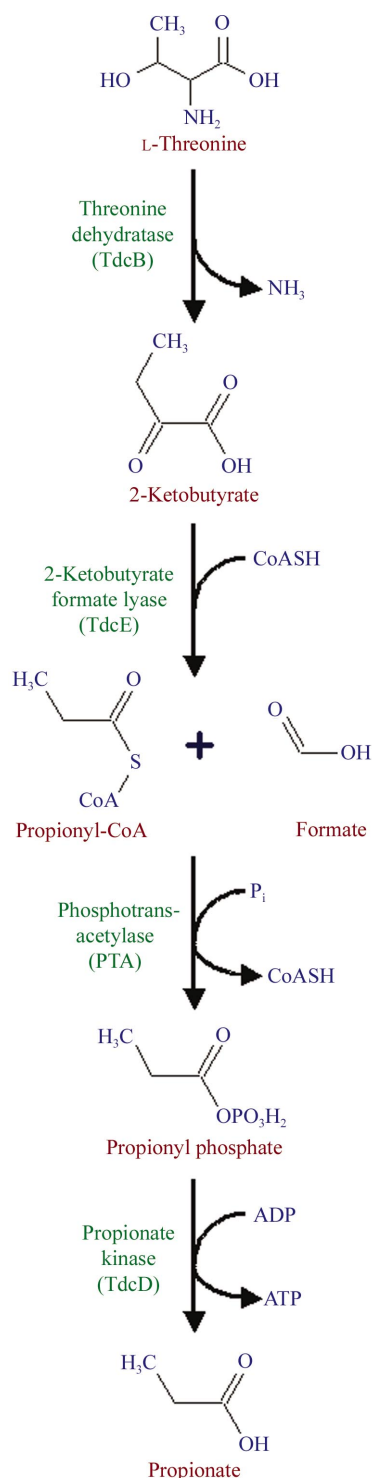


Figure 1
Pathway for anaerobic degradation of L-threonine to propionate via 2-ketobutyrate.

identity of 38% to *Methanosarcina thermophila* acetate kinase. In *E. coli*, it has been shown to also possess acetate kinase (AckA) activity (Hesslinger *et al.*, 1998) and the two enzymes are therefore likely to have similar structures and catalytic mechanisms. The crystal structure of acetate kinase from *Methanosarcina thermophila* has been determined (Buss *et al.*, 2001). Despite the absence of sequence identity, the fold of acetate kinase contains a core that is similar to those of the glycerol kinase/hexokinase/actin/Hsc70 superfamily. The fold consists of a duplicated $\beta\beta\alpha\beta\alpha\beta\alpha\beta$ secondary structure with insertions of subdomains between particular β -sheet elements. The literature provides evidence for two contrasting mechanisms of acetate kinase function. Acetate kinase becomes phosphorylated in the presence of acetyl phosphate or ATP (Todhunter & Purich, 1974) and the stable phosphoenzyme can be isolated (Anthony & Spector, 1970, 1972; Fox & Roseman, 1986). The phosphoenzyme is able to transfer the phosphoryl group to either ADP or acetate, suggesting that the enzyme-linked covalent intermediate is involved in catalysis. On the other hand, *E. coli* acetate kinase has been shown to transfer the phosphoryl group with inversion of configuration (Blättler & Knowles, 1979), suggesting that the transfer takes place directly from the substrate to the product without the formation of an enzyme-linked covalent intermediate.

In this paper, we report the cloning, high-level expression, purification and preliminary X-ray crystallographic studies of propionate kinase encoded by the *tdcD* gene from *S. enterica* serovar *Typhimurium* strain IFO12529. Structure determination of propionate kinase will provide catalytic insight into this particular protein and allow direct structural comparison with acetate kinase and other members of this superfamily.

2. Materials and methods

2.1. Cloning and expression

The *tdcD* gene was PCR-amplified from *S. enterica* serovar *Typhimurium* genomic DNA using KOD HiFi DNA polymerase (Novagen). After amplification of the target gene by sense 5'-CATGCCATGGCTAGCAATGAATTTCCGGTCG-3' and anti-sense 5'-CGGGATCCTTACTCGAGTGCAAATTCCTACTGG-3' primers, the PCR-amplified fragment was digested with *NheI* and *BamHI* and then cloned into the vector pRSET-C (Invitrogen) encoding a polypeptide with an N-terminal hexahistidine tag to facilitate purification. TdcD protein was expressed in the host strain *E. coli* BL21 (DE3) plysS. Expression was performed in 1 l Terrific Broth medium, which was incubated at 310 K until the OD₆₀₀ reached about 0.6. TdcD expression was induced by the addition of 0.3 mM isopropyl β -D-thiogalactopyranoside (IPTG) for an additional 4 h at 303 K. For the preparation of soluble protein fractions, cells from 1 l culture were first pelleted and then resuspended in 50 ml cold lysis buffer containing 50 mM Tris pH 8.0, 200 mM NaCl. It was then lysed by sonication on ice. The clear supernatant containing soluble protein was collected by centrifugation. All the following purification steps were performed at 277 K.

2.2. Purification

TdcD with an N-terminal hexahistidine tag was purified using Ni-NTA His-bind resin (Novagen). Once all unbound proteins had been washed from the column using 50 mM Tris pH 8.0, 200 mM NaCl and 10–20 mM imidazole, TdcD protein was eluted from the column using 200 mM imidazole along with 50 mM Tris pH 8.0, 200 mM NaCl. In order to remove the imidazole, the protein was extensively dialysed against 25 mM Tris pH 8.0, 50 mM NaCl, 5 mM MgCl₂ and 1 mM

Table 1

Data-collection statistics.

Values in parentheses correspond to the last resolution shell.

Wavelength (Å)	1.542
Resolution range (Å)	50.0–2.2
Space group	<i>P</i> 3 ₁ 21
Temperature (K)	100
Unit-cell parameters (Å)	
<i>a</i> = <i>b</i>	111.47
<i>c</i>	66.52
Total No. reflections	515571
No. unique reflections	24553
Completeness (%)	99.8 (98.2)
Multiplicity	5.9 (4.9)
Molecules per AU	1
<i>V</i> _M (Å ³ Da ⁻¹)	2.7
Solvent content (%)	53.2
Average <i>I</i> / σ (<i>I</i>)	10.9 (3.5)
<i>R</i> _{merge} [†] (%)	6.5 (46.9)

[†] $R_{\text{merge}} = \sum |I_j - \langle I_j \rangle| / \sum \langle I_j \rangle$, where *I_j* is the intensity of reflection *j* and $\langle I_j \rangle$ is the average intensity of reflection *j*.

DTT. Dialysed protein was concentrated to a final concentration of 10 mg ml⁻¹ using a 30 kDa molecular-weight cutoff Centricon (Vivaspin). TdcD was obtained with a final yield of 25 mg per litre of cell culture. The purity of the protein was estimated using SDS-PAGE and was found to be nearly homogeneous (Fig. 2). The sequence of the *tdcD* gene was determined by nucleotide sequencing and confirmed by comparing it with the *tdcD* gene of *S. typhimurium* LT2.

2.3. Crystallization

Initial crystallization experiments were carried out by the hanging-drop vapour-diffusion and microbatch methods using Crystal Screens I and II and Index Screen from Hampton Research. Prior to crystallization, the TdcD protein was incubated with 5 mM ADP and 25 mM propionate for 12 h at 277 K. Crystallization drops were

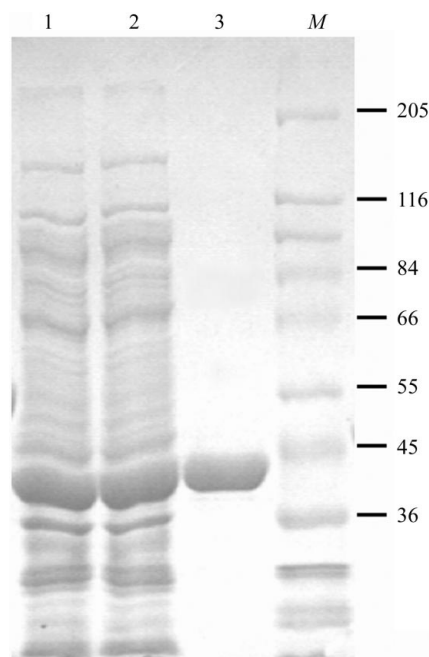


Figure 2
SDS-PAGE analysis of TdcD during purification. Proteins were analysed on 10% SDS-PAGE and stained with Coomassie blue. Lane 1, crude cell lysates after 0.3 mM IPTG induction; lane 2, clear supernatant; lane 3, purified TdcD after Ni-NTA affinity column chromatography; lane *M*, molecular-weight markers (kDa).

prepared by mixing 4 μ l protein solution with 3 μ l reservoir solution and were suspended over 500 μ l reservoir solution in a hanging-drop vapour-diffusion setup. In the microbatch method, 4 μ l protein solution and 3 μ l crystallization reagent were pipetted under a layer of paraffin oil and silicon oil in a 1:1 ratio (Hampton Research). Diffraction-quality crystals were obtained at 291 K in condition No. 57 [0.05 M ammonium sulfate, 0.05 M bis-tris pH 6.5, 30% pentaerythritol ethoxylate (15/4 EO/OH)] and condition No. 46 [0.1 M bis-tris pH 6.5, 20% polyethylene glycol monomethyl ether (PEG MME) 5000] of the Index Screen from Hampton Research. Further optimization of the latter condition with different molecular weights of PEG MME at various concentrations gave good diffraction-quality crystals using 12% PEG MME 5000, 18% PEG MME 2000 or 20% PEG MME 550 in the presence of 0.1 M bis-tris pH 6.5. These crystals appeared after 5 d equilibration against the crystallization solution and grew to full size in 10 d (Fig. 3).

2.4. Data collection

Crystals were transferred to a cryoprotectant composed of reservoir solution with 20% ethylene glycol. X-ray diffraction data were collected from a single crystal using a MAR Research image-plate system (diameter 345 mm) with Osmic mirrors and a Rigaku RU-200

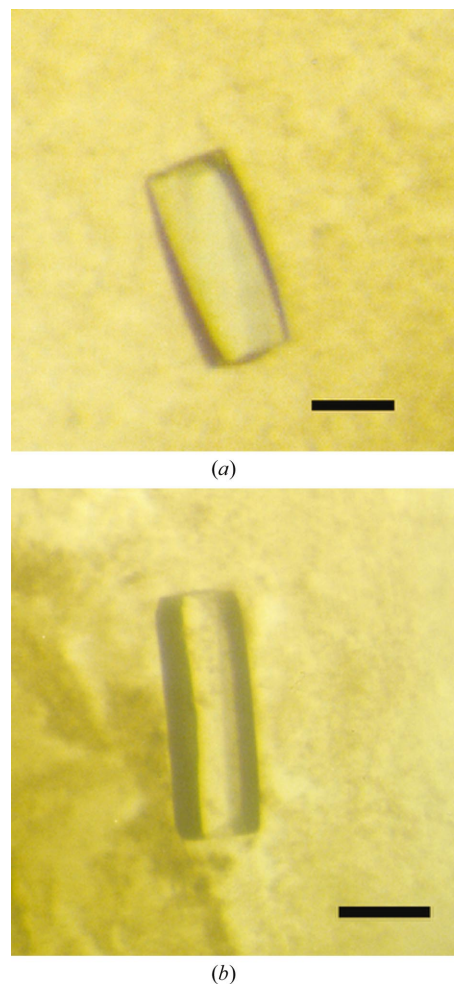


Figure 3
Crystals of TdcD protein from *S. typhimurium* obtained from (a) a microbatch setup using 0.05 M ammonium sulfate, 0.05 M bis-tris pH 6.5, 30% pentaerythritol ethoxylate (15/4 EO/OH) and (b) a hanging-drop vapour-diffusion setup using 0.1 M bis-tris pH 6.5, 18% polyethylene glycol monomethyl ether 2000. The scale bar represents 0.1 mm.

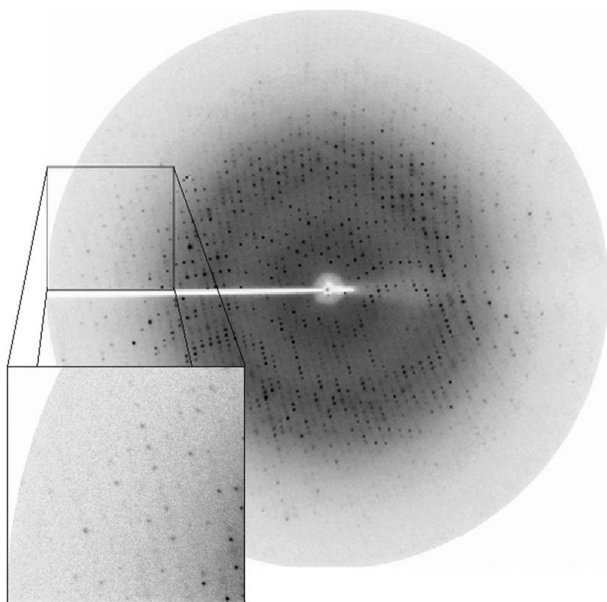


Figure 4

A typical 0.5° oscillation image obtained during data collection from a TdcD crystal. The edge of the oscillation image corresponds to 2.18 Å resolution.

rotating-anode X-ray generator with a 300 µm focal cup. The crystal-to-detector distance was set to 195 mm. All frames were collected at 100 K using a 0.5° oscillation angle, with an exposure time of 480 s per frame. The data revealed significant diffraction to 2.2 Å resolution. The data were processed with *DENZO* and *SCALEPACK* (Otwinowski & Minor, 1997). A data-quality program (Diederichs & Karplus, 1997) was used to evaluate the data quality. The final statistics for data collection and processing are summarized in Table 1.

3. Results and discussion

The hanging-drop and microbatch methods both gave good diffraction-quality crystals. Crystals obtained from various conditions were of the same crystal form. Crystals obtained from condition No. 57 diffracted better than those obtained from other conditions and a complete diffraction data set was collected to 2.2 Å resolution from a single crystal (Fig. 4). Systematic absences showed that the crystal belongs to space group *P*3₁21 or *P*3₂21. The volume of the asymmetric unit of the crystal is compatible with only one subunit, with a

volume per unit molecular weight of the protein of 2.7 Å³ Da⁻¹ and a calculated solvent content of 53.2% (Matthews, 1968). A preliminary solution of the structure of propionate kinase was obtained by molecular-replacement calculations using the crystal structure of acetate kinase (PDB code 1g99) from *M. thermophila* (Buss *et al.*, 2001) as the search model using the *AMoRe* program (Navaza, 1994). To ascertain the correct space group, both enantiomorphs were tested. The best results were obtained with space group *P*3₁21, giving a correlation coefficient of 37.4% and an *R* factor of 51.6% at 15–3.5 Å resolution. Examination of the best solution revealed good crystal packing and no clashes between symmetry-related molecules. This preliminary model is currently being refined.

The intensity data were collected at the X-ray Facility for Structural Biology at the Indian Institute of Science, supported by the Department of Science and Technology (DST) and the Department of Biotechnology (DBT). We thank Sagar Chittori and Professor H. S. Savithri for useful discussions. DKS would like to thank CSIR, India for offering financial support.

References

- Anthony, R. S. & Spector, L. B. (1970). *J. Biol. Chem.* **246**, 6730–6741.
 Anthony, R. S. & Spector, L. B. (1972). *J. Biol. Chem.* **247**, 2120–2125.
 Blättler, W. A. & Knowles, J. R. (1979). *Biochemistry*, **18**, 3927–3933.
 Buss, K. A., Cooper, D. R., Ingram-Smith, C., Ferry, J. G., Sanders, D. A. & Hasson, M. S. (2001). *J. Bacteriol.* **183**, 680–686.
 Datta, P., Goss, T. J., Omnaas, J. R. & Patil, R. V. (1987). *Proc. Natl Acad. Sci. USA*, **84**, 393–397.
 Diederichs, K. & Karplus, P. A. (1997). *Nature Struct. Biol.* **4**, 269–275.
 Fox, D. K. & Roseman, S. (1986). *J. Biol. Chem.* **261**, 13487–13497.
 Ganduri, Y. L., Satta, S. R., Datta, M. W., Jambukeswaran, R. K. & Datta, P. (1993). *Mol. Gen. Genet.* **240**, 395–402.
 Hesslinger, C., Fairhurst, S. A. & Sawers, G. (1998). *Mol. Microbiol.* **27**, 477–492.
 Matthews, B. W. (1968). *J. Mol. Biol.* **33**, 491–497.
 Navaza, J. (1994). *Acta Cryst.* **A50**, 157–163.
 Otwinowski, Z. & Minor, W. (1997). *Methods Enzymol.* **276**, 307–326.
 Sawers, G. (1998). *Arch. Microbiol.* **171**, 1–5.
 Sawers, G. (2001). *Mol. Microbiol.* **39**, 1285–1298.
 Schweizer, H. P. & Datta, P. (1988). *J. Bacteriol.* **170**, 5360–5363.
 Sumantran, V. N., Schweizer, H. P. & Datta, P. (1990). *J. Bacteriol.* **172**, 4288–4294.
 Tokushige, M., Whiteley, H. R. & Hayaishi, O. (1963). *Biochem. Biophys. Res. Commun.* **13**, 380–385.
 Todhunter, J. A. & Purich, D. L. (1974). *Biochem. Biophys. Res. Commun.* **60**, 273–280.
 Van Dyk, T. K. & LaRossa, R. A. (1987). *Mol. Gen. Genet.* **207**, 435–440.